

## Supplementary Information

# **Precrystalline P3HT nanowires: growth-controllable solution processing and effective molecular packing transfer to thin-film**

Seon-Mi Jin,<sup>a</sup> Jun Ho Hwang,<sup>a</sup> Jung Ah Lim<sup>\*b</sup> and Eunji Lee<sup>\*a</sup>

Corresponding Authors

E-mail: [jalim@kist.re.kr](mailto:jalim@kist.re.kr) and [eunjilee@gist.ac.kr](mailto:eunjilee@gist.ac.kr)

<sup>a</sup>School of Materials Science and Engineering, Gwangju Institute of Science and Technology (GIST), Gwangju 61005, Republic of Korea

<sup>b</sup>Center for Opto-Electronic Materials and Devices, Korea Institute of Science and Technology (KIST), Seoul 02792, Republic of Korea

**1. Materials and Instruments** All commercially available reagents were used without further purification unless otherwise indicated. 1,2-Bis(diphenylphosphinoethane)nickel(II) chloride [Ni(dppp)Cl<sub>2</sub>] was purchased from Aldrich Chemical Co., Ltd., and palladium(II) acetate [Pd(OAc)<sub>2</sub>] was purchased from Kawaken Fine Chemicals Co., Ltd., Bis(triphenylphosphine)nickel(II) chloride [(PPh<sub>3</sub>)<sub>2</sub>NiCl<sub>2</sub>] was purchased from TCI Chemical Co., Ltd., and stored in a vacuum atmosphere glovebox under N<sub>2</sub>.

**Nuclear magnetic resonance spectroscopy (NMR).** All <sup>1</sup>H NMR spectra were recorded at 500 MHz, using CDCl<sub>3</sub> as a solvent, unless otherwise stated. The chemical shifts of all <sup>1</sup>H NMR spectra are referenced to the residual signal of CDCl<sub>3</sub> ( $\delta$  7.26 ppm) by Bruker 500 MHz NMR instrument. All coupling constants, *J*, are reported in Hertz (Hz).

**Gel permeation chromatography (GPC).** GPC measurements were performed on a Waters RI system equipped with a UV detector, a differential refractometer detector, and an Ultrastyrigel linear column at 35 °C using THF as the eluent. The molecular weight (*M<sub>w</sub>*) and the polydispersity index (PDI) were calculated using monodisperse polystyrene standards.

**Ultraviolet-visible (UV-Vis) spectroscopy.** Absorption spectra were obtained using UV-Vis spectrometer (UV-1800, Shimadzu, Japan).

**Transmission electron microscopy (TEM).** TEM specimens were prepared by 2  $\mu$ L drop of the P3HT solution onto a carbon-coated copper grid, and excess solvent was removed by a piece of paper. The images were obtained with dried specimens using a JEOL JEM-1400 (JEOL Ltd., Tokyo, Japan) at an accelerating voltage of 120 kV, and the images were acquired with a SC 1000 CCD camera (Gatan, Warrendale, PA).

## **2. Methods**

**Crystallization-driven self-assembly of P3HT.** Three different kinds of solution processes using the different mixing solvents, including solution-biphase (SBM), dropwise addition (DAM), and one-pot addition (OAM) methods, are used for the crystallization of poly(3-hexylthiophene) (P3HT). The crystallization-driven assembly is induced by the addition of orthogonal solvent to the good solvent for P3HT. Chloroform (CF) was selected as a good solvent, while dichloromethane (DCM), hexane (HEX), acetonitrile (ACN), and methanol (MeOH) were used as marginal-, poor-, and non-solvents.

- **SBM:** The orthogonal solvent was injected into P3HT CF solution along the vial wall with a syringe to gradually induce the mutual interaction between P3HT and orthogonal solvent. The

crystallization-driven self-assembly of P3HT occurs at the interface between good and orthogonal solvent layers. The orthogonal solvent progressively diffused into CF to promote P3HT crystallization.

- **DAM:** The syringe pump was used for dropwise addition of orthogonal solvent with the rate of 100  $\mu\text{L min}^{-1}$  into P3HT CF. The added solvent was mixed under stirring.
- **OAM:** Rapid one-pot injection of orthogonal solvent was carried out with 1 mL pipette into P3HT CF to promote the aggregation between P3HT chains.

**Quantitative analysis of aggregated P3HT chains.** The absorption spectra of each solution were normalized to the peak of the 0-2 vibronic transition.<sup>S1,S2</sup> The measured absorption spectra are composed of a high-energy region attributed to unaggregated P3HT chains and a low-energy region originated from the vibronic structure of aggregated P3HT chains. The absorption spectrum was decomposed into a scaled unaggregated P3HT chains in CF (gray dot line), and aggregate spectrum (colour dash-dot line). The spectrum of unaggregated chains in CF (gray dot line) was subtracted from the original spectrum (respective open symbol, solid line) containing both aggregated and unaggregated chains, resulting in the spectrum representing the dash-dot line, as shown in Fig. S4 and S6. The equation is below.

$$f(x) = \frac{1}{\sqrt{2\pi}\sigma} e^{-\frac{(x-\mu)^2}{2\sigma^2}} \quad \int_{-\infty}^{\infty} f(x) dx = 1 \quad (1)$$

In order to analyze the aggregation of P3HT, the relative intensity between the vibronic transitions in the absorption spectra of the P3HT solution was compared within the weak interchain coupling framework model developed by Clark et al.<sup>S3</sup> The ratio of the  $A_{0-0}$  and  $A_{0-1}$  absorbance is related to the free exciton bandwidth ( $W$ ) of the aggregates and the energy of the main intramolecular vibration energy ( $E_p$ ) coupled to the electronic transition by the following expression (assuming a Huang-Rhys factor of 1):

$$\frac{A_{0-0}}{A_{0-1}} = \left( \frac{1 - 0.24W/E_p}{1 + 0.073W/E_p} \right)^2 \quad (2)$$

Using the  $A_{0-0}/A_{0-1}$  ratio from equation, and assuming the C=C symmetric stretch at 0.179 eV dominates the coupling to the electronic transition,  $W$  can be estimated. If the intensity ratio of the  $A_{0-0}/A_{0-1}$  is smaller than 1, it is the H-type aggregation model.

### 3. Synthesis

**Synthesis of poly(3-hexylthiophene) (P3HT).** Lithium diisopropylamide (LDA) was generated by addition of *n*-BuLi (2.5 M in hexane, 2.31 mL, 5.77 mmol) to a solution of diisopropylamine (1.02 mL, 7.28 mmol) in dry THF (14.6 mL, 0.5 M conc.) at -78 °C. The solution was stirred at this temperature for 1 h. The freshly generated LDA solution was added dropwise to the 2-bromo-3-hexylthiophene (1.50 g, 6.068 mmol) in dry THF (45 mL) at -78 °C. After 1 h, ZnCl<sub>2</sub> (868 mg, 6.37 mmol) was added portionwise to the mixture, which was stirred for 30 min and then warmed slowly to room temperature. Polymerization initiated by addition of Ni(dppp)Cl<sub>2</sub> (65.79 mg, 0.121 mmol) to the mixture was carried out at room temperature for 20 min. The polymer was precipitated with methanol, and the resulting precipitate was then filtered. Oligomers and impurities in the product were removed by soxhlet extractions with methanol and hexane, followed by chloroform extraction. The polymer was recovered from the chloroform fraction, followed by concentration and finally precipitation into methanol. <sup>1</sup>H NMR (500 MHz, CDCl<sub>3</sub>) δ 6.98 (s, 1H), 2.69-2.86 (m, 2H), 1.55-1.65 (m, 2H), 1.35-1.48 (m, 2H), 1.22-1.40 (m, 4H), 0.90 (t, *J* = 6.2 Hz, 3H).

**Table S1** Characteristics of synthesized P3HT homopolymers

Polymer	$M_n(\text{g mol}^{-1})^a$	$M_g(\text{g mol}^{-1})^a$	PDI <sup>a</sup>	regioregularity <sup>b</sup>
P3HT (12.7K)	12,700	15,400	1.21	92%
P3HT (7.3K)	7,300	8,400	1.16	91%

<sup>a</sup>Determined from GPC in THF calibrated by polystyrene standards; <sup>b</sup>From <sup>1</sup>H NMR.

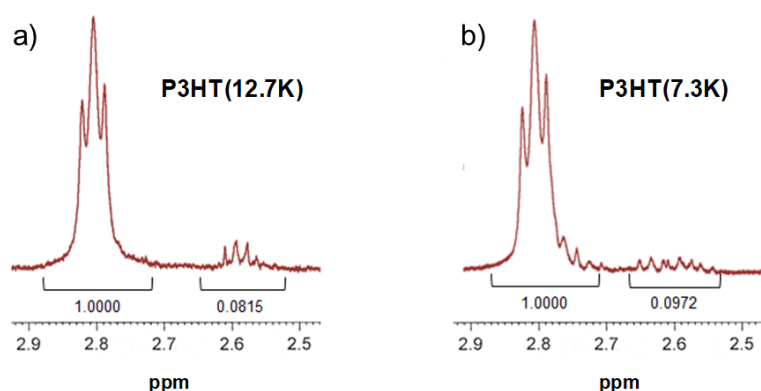


**Fig. S1** Expanded region from <sup>1</sup>H NMR of (a) P3HT (12.7K) and (b) P3HT (7.3K) representing the regiochemistry of P3HT.

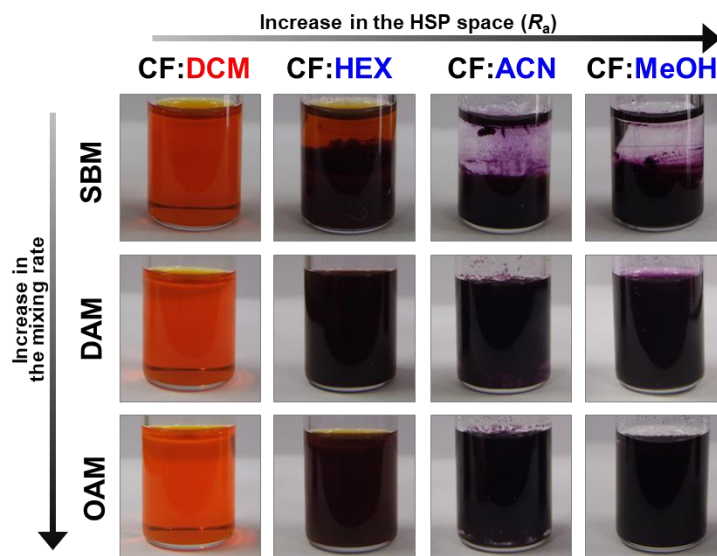


**Fig. S2** Photographs of P3HT (12.7 K) in 1:1 (v/v) mixed solutions of CF and each orthogonal solvent (DCM as a marginal solvent, HEX as a poor solvent, ACN and MeOH as a non-solvent;  $0.5 \text{ mg mL}^{-1}$ ) according to the mixing rates of good and orthogonal solvents. All photographs were captured after aging for 1 day.

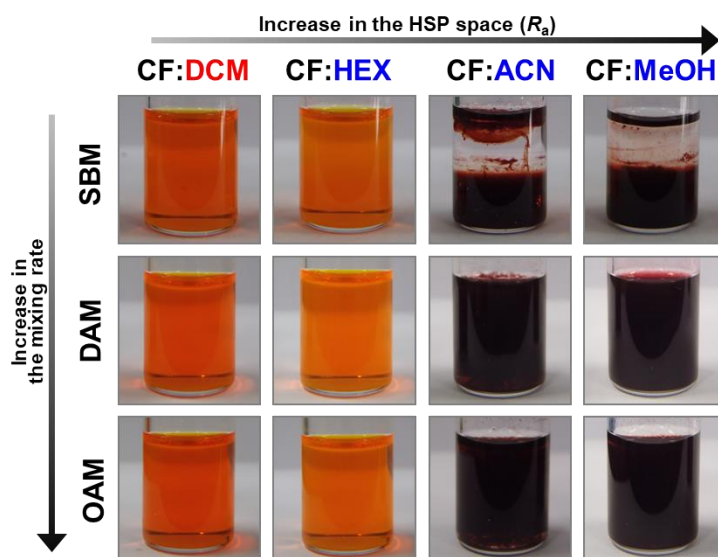


**Fig. S3** Photographs of P3HT (7.3K) in 1:1 (v/v) mixed solutions of CF and each orthogonal solvent (DCM, HEX, ACN, and MeOH;  $0.5 \text{ mg mL}^{-1}$ ) according to mixing rates of good and orthogonal solvents. All photographs were captured after aging for 1 day.

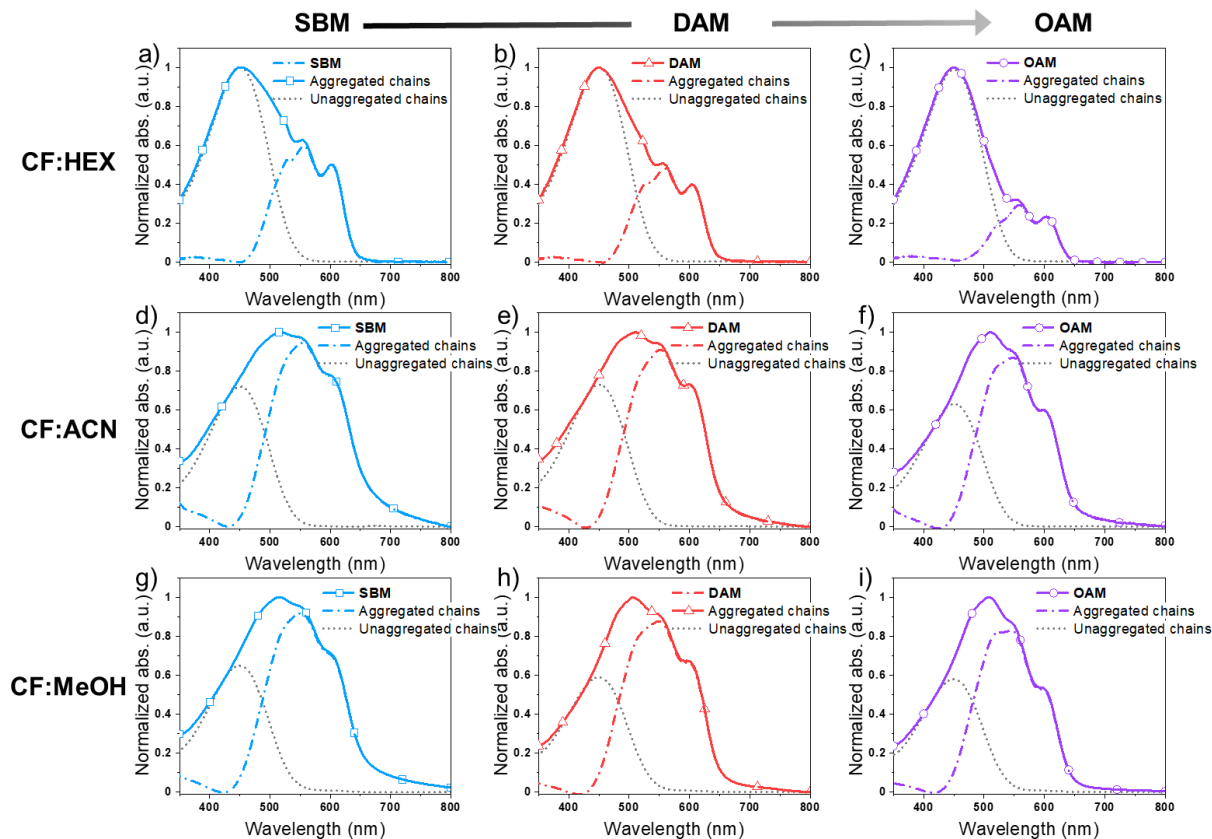


**Fig. S4** Experimental absorption spectra normalized to 0-2 absorption strength for P3HT (12.7K) solution in (a-c) CF:HEX, (d-f) CF:ACN, and (g-i) CF:MeOH according to mixing methods (including SBM, DAM, and OAM). Each absorption spectrum was decomposed into a scaled unaggregated P3HT in CF (gray dot line) and aggregated P3HT in solvent mixture (colour dash-dot line).

**Table S2** The fraction of aggregated P3HT (12.7K) chains and their free-exciton bandwidth ( $W$ ) calculated from the absorption spectra of Fig. S4 according to the mixing methods (SBM, DAM, and OAM)

Mixing Method	CF:HEX		CF:ACN		CF:MeOH	
	Aggregated chains (%)	$W^a$ [Free-exciton bandwidth, eV]	Aggregated chains (%)	$W^a$ [Free-exciton bandwidth, eV]	Aggregated chains (%)	$W^a$ [Free-exciton bandwidth, eV]
SBM	36.5	0.059	62.2	0.068	63.1	0.083
DAM	31.4	0.068	59.7	0.077	62.7	0.085
OAM	21.9	0.088	59.5	0.115	60.6	0.137

<sup>a</sup>Determined by using Spano's model for weakly interacting H-aggregates.<sup>S4</sup>

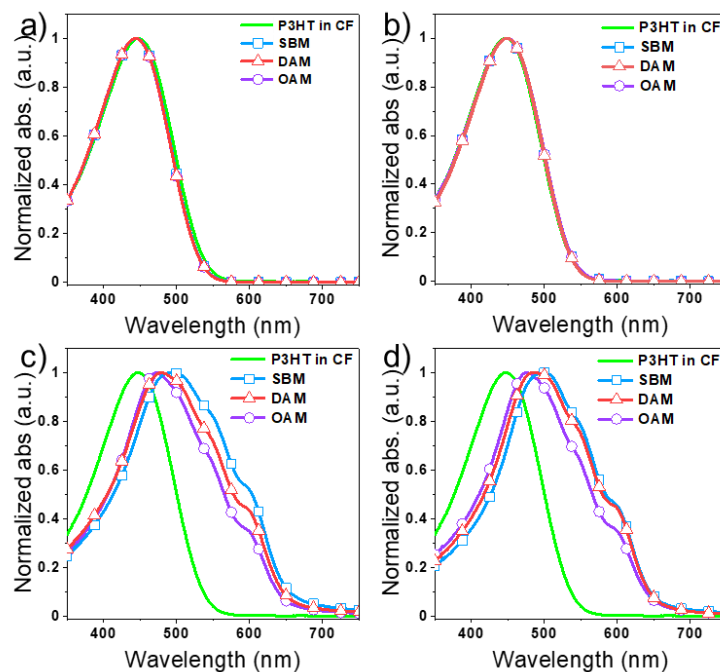


**Fig. S5** Normalized absorption spectra of P3HT (7.3K) in (a) CF:DCM, (b) CF:HEX, (c) CF:ACN, and (d) CF:MeOH (1:1, v/v; 0.1 mg mL<sup>-1</sup>) according to the mixing methods (SBM, DAM, and OAM).

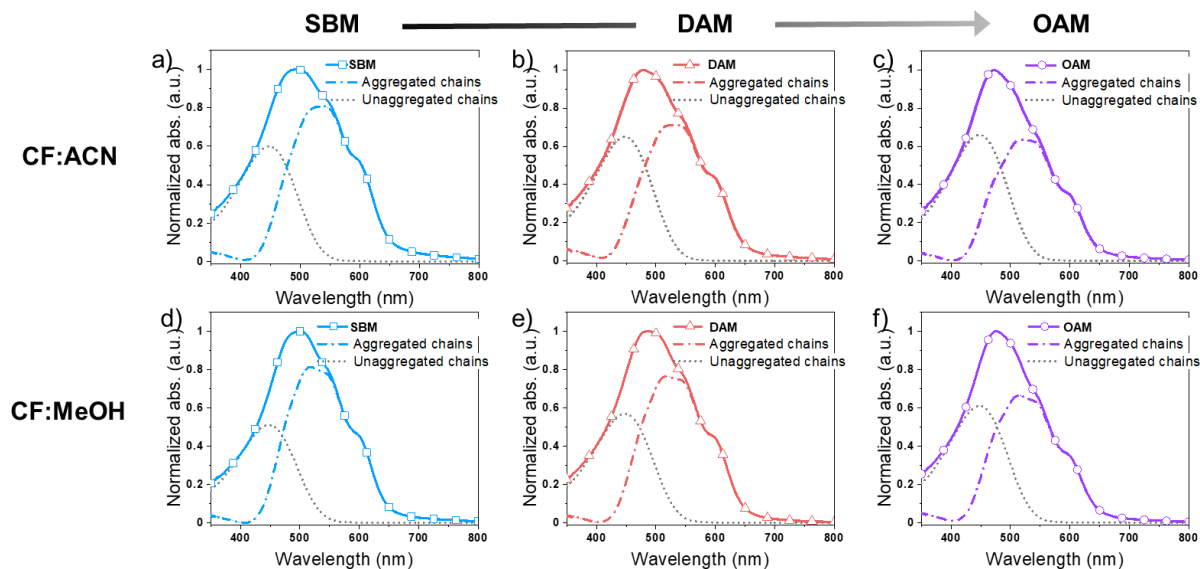


**Fig. S6** Experimental absorption spectra normalized to 0-2 absorption strength for P3HT (7.3K) solution in (a-c) CF:ACN and (d-f) CF:MeOH according to the mixing methods (including SBM, DAM, and OAM). Each absorption spectrum was decomposed into a scaled unaggregated P3HT in CF (gray dot line) and aggregated P3HT in solvent mixture (colour dash-dot line).

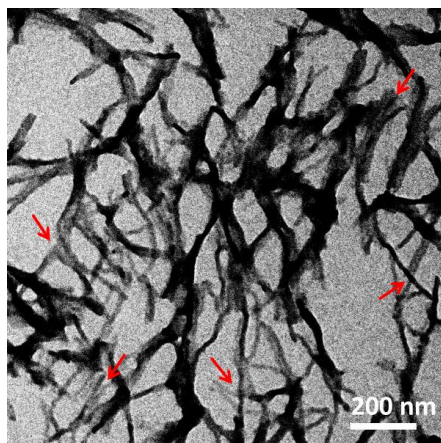


**Fig. S7** TEM image of P3HT (12.7K) NW-networks formed by SBM using CF:ACN (1:1, v/v).

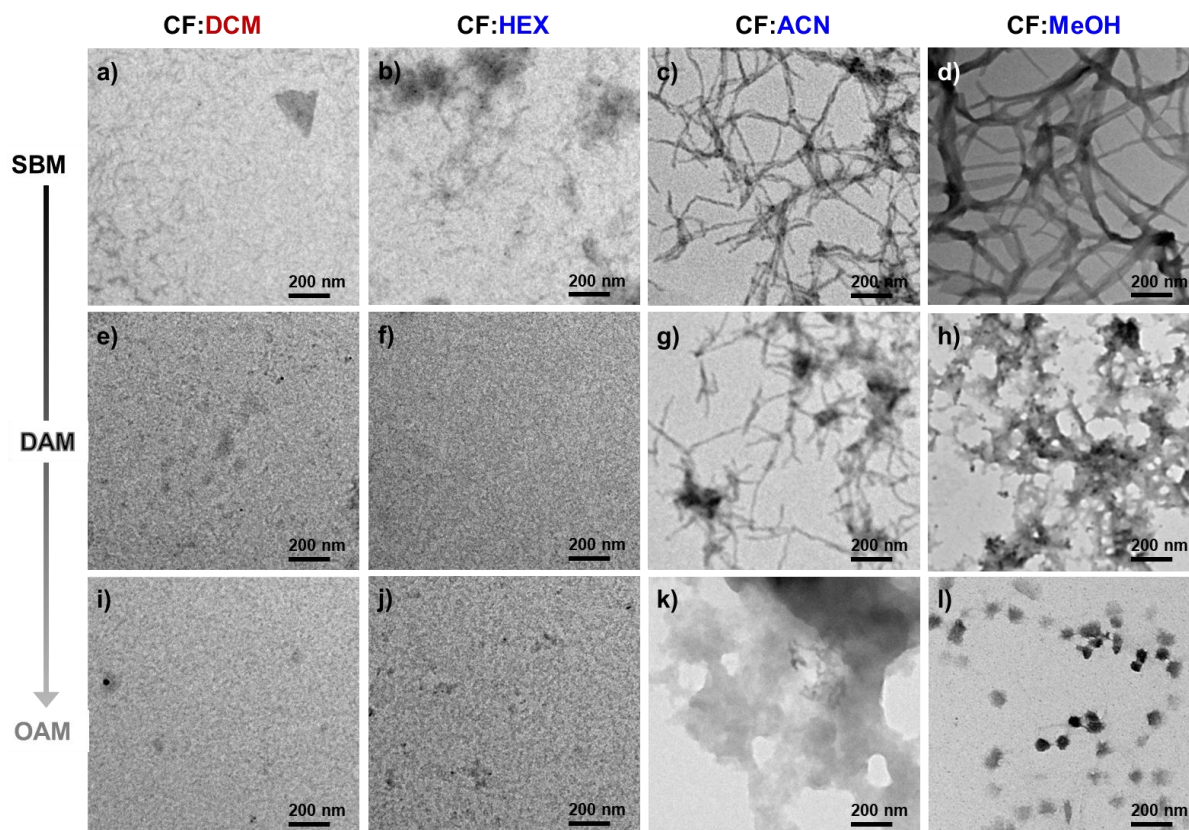


**Fig. S8** (a-l) TEM images of each self-assembled P3HT (7.3K) aggregate processed from (a-d) SBM, (e-h) DAM, and (i-l) OAM ( $0.5 \text{ mg mL}^{-1}$ ). The binary mixed solvent systems were (a,e,i) CF:DCM, (b,f,j) CF:HEX, (c,g,k) CF:ACN, and (d,h,l) CF:MeOH.



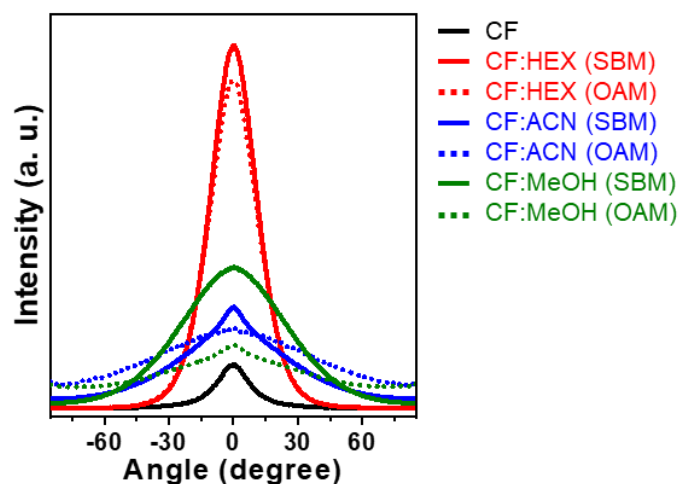


**Fig. S9** Azimuthal distributions of the (100) peak intensity. 2D GI-WAXS patterns of thin-films as-cast from solutions containing P3HT (12.7K). The solid and dotted lines indicate the distributions from SBM and OAM, respectively.

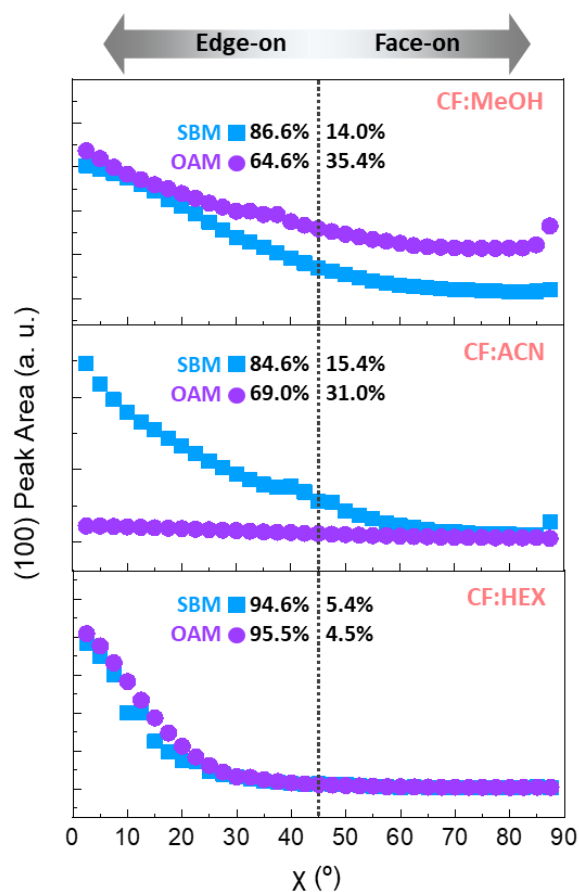


**Fig. S10** Plot figures obtained at (100) scattering peaks of P3HT (12.7K). The figures were described without calibration with geometric factor, but the calculation of the relative ratio of the edge-on and face-on crystallite orientation was examined after correction with a geometric factor.<sup>S5,S6</sup>

**Table S3** The orientation of crystallites of P3HT (12.7K) in each solvent condition at (100) peak

Solvent conditions	SBM		OAM	
	(100) peak Edge-on (%) <sup>a</sup>	(100) peak Face-on (%) <sup>a</sup>	(100) peak Edge-on (%) <sup>a</sup>	(100) peak Face-on (%) <sup>a</sup>
CF:HEX	94.6	5.4	95.5	4.5
CF:ACN	84.6	15.4	69.0	31.0
CF:MeOH	86.0	14.0	64.6	35.4

<sup>a</sup>Determined from pole figure of (100) scattering peaks after correction with geometric factor. The fraction of orientation was estimated to be the relative ratios of the integrated area at azimuthal angle, 0°-45° and 45°-90°. <sup>55,56</sup>

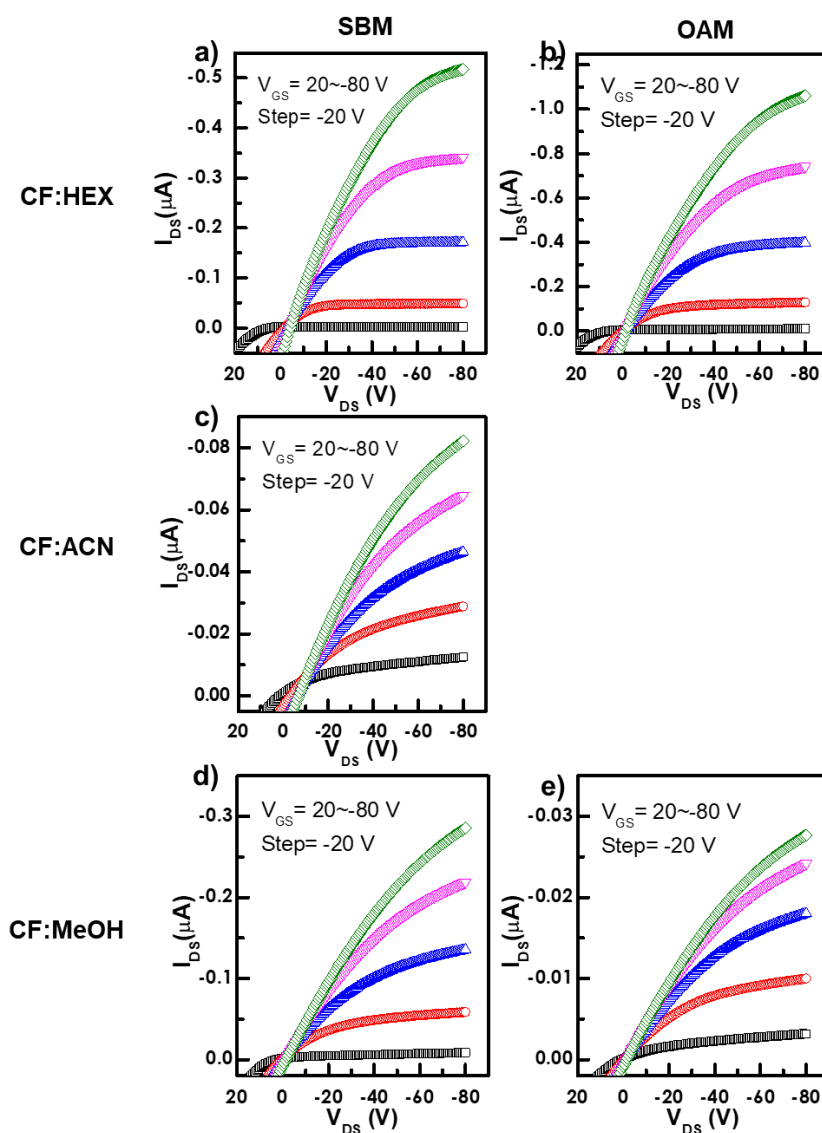


**Fig. S11** Output ( $I_{DS} - V_{DS}$ ) characteristics of P3HT (12.7K) thin-film transistor fabricated as-cast from the P3HT solution prepared by (a,c,d) SBM and (b,e) OAM in 1:1 (v/v) mixed solvent of (a,b) CF:HEX, (c) CF:ACN, and (d,e) CF:MeOH.

## References

- S1. C. Scharsich, R. H. Lohwasser, M. Sommer, U. Asawapirom, U. Scherf, M. Thelakkat, D. Neher, A. Köhler, *J. Polym. Sci. Part B: Polym. Phys.*, 2012, **50**, 442-453.
- S2. G. Nagarjuna, M. Baghgar, J. A. Labastide, D. D. Algaier, M. D. Barnes, D. Venkataraman, *ACS Nano*, 2012, **6**, 10750-10758.
- S3. J. Clark, J.-F. Chang, F. C. Spano, R. H. Friend, C. Silva, *Appl. Phys. Lett.*, 2009, **94**, 163306.
- S4. F. C. Spano, *J. Chem. Phys.*, 2005, **122**, 234701.
- S5. J. Rivnay, R. Steyrleuthner, L. H. Jimison, A. Casadei, Z. Chen, M. F. Toney, A. Facchetti, D. Neher, A. Salleo, *Macromolecules*, 2011, **44**, 5246-5255.
- S6. G. Kim, S. J. Kang, G. K. Dutta, Y. K. Han, T. J. Shin, Y.-Y. Noh, C. Yang, *J. Am. Chem. Soc.*, 2014, **136**, 9477-9483.